Nano-ZnO-loaded poly (acrylamide-co-itaconic acid) hydrogel as adsorbent for effective removal of iron from contaminated water

Neeraj Sharma, Alka Tiwari*

*Department of Chemistry, Govt. V.Y.T. PG. Autonomous College, Durg, CG 491001, India, Tel. +91 9098190861;
email: neeraj.sharma.shyam@gmail.com (N. Sharma), Tel. +91 7415514000; Fax: +91 788 2324783; emails: brnsbarc18@gmail.com,
alkatiwari18@yahoo.co.in (A. Tiwari)*

ABSTRACT

The present research focuses on the adsorptive efficiency of nano-ZnO-loaded poly (acrylamide-co-itaconic acid) hydrogel for iron removal from synthetic as well as contaminated water by batch and column adsorption techniques. The influence of pH, contact time, adsorbent dose, temperature, and metal ion concentration on the sensitivity of the removal process was inspected. The copolymer was synthesized and nano-ZnO particles were incorporated within the polymeric matrix by in situ technique. The size, structure, and coating of nano-ZnO particles were characterized by TEM, SEM, Fourier transform infrared spectroscopy, and AFM analysis, respectively. The sorption data were analyzed and fitted to linearized adsorption isotherm of the Langmuir, Freundlich, and Temkin equations, respectively. Equilibrium data fitted very well to the Freundlich model. The kinetics of sorption was analyzed using pseudo-first-order and pseudo-second-order kinetic models. Kinetic parameters, rate constants, equilibrium sorption capacities, and related correlation coefficients for each kinetic model were calculated. Different thermodynamic parameters, i.e. $\Delta G°$, $\Delta H°$ and $\Delta S°$ were also evaluated which proved the sorption to be feasible, spontaneous, and exothermic in nature. This hydrogel has been found to be an efficient adsorbent for iron removal from water (>99% removal) and could be regenerated efficiently for further experiments.

Keywords: Nano-ZnO particles; Hydrogel; Isotherms; Kinetics; Thermodynamics

1. Introduction

Discharge of toxic and polluting heavy metal ions from industrial and municipal wastewater into rivers and streams is an important factor which affects environmental water quality [1]. Pollution of natural water resources due to toxic heavy metals is a serious environmental problem, nowadays as they are introduced into the environment through a variety of natural and anthropogenic pathways [2]. The quality of water is initially concerned for mankind since it is directly linked with human welfare [3]. The toxic effects of heavy metals affect not only the ecosystem, but also human beings through bioaugmentation and bioaccumulation in the food chain [4]. These wastewaters need to be treated before being discharged into natural environment for the protection of natural resources and human health [5].

About 80% of communicable diseases in the world are waterborne. Among various naturally occurring

*Corresponding author.

and undesirable pollutants in water bodies, iron, arsenic, fluoride, lead, cadmium, and mercury are very important as they cause severe health problems [6]. Iron is a natural constituent of the earth's crust and is present in varying concentrations in all ecosystems [7]. Iron is a key element in industries and plays a vital role in health, science technology, and metallurgy [8]. Iron is stable and persistent environmental contaminant since it cannot be destroyed or degraded. The presence of iron in natural water may be attributed to the dissolution of rocks and minerals, acid mine drainage, landfill leachate, steel producing industries, sewage, or industrial effluents. Iron exists in two forms, soluble ferrous iron (Fe^{2+}) and insoluble ferric particulate iron (Fe^{3+}). WHO recommended guideline value for iron in drinking water is $0.3 \, mg \, dm^{-3}$ and the maximum permissible limit is $1 \, mg \, dm^{-3}$.

Iron toxicity causes many health problems in human beings. Our body can excrete iron to a limited extent so it may easily be stored in different organs like heart, liver, and pancreas. Storage of iron in organs is dangerous because iron acts as a potent oxidizer and may damage our body tissues, which contribute to serious health hazards like liver cancer, cardiac arrhythmias, cirrhosis, diabetes, Alzheimer's disease, anorexia, diarrhea, hypothermia, metabolic acidosis, damage of gastrointestinal tract, bacterial and viral infections, and even death.

Adsorption, ion exchange, reverses osmosis, distillation, coagulation, and chemical precipitation are some treatment techniques for the removal of iron from water. However, most of this method might not be efficient in removing heavy metals at very low concentrations and could be relatively expensive. These methods are also not effective due to their secondary effluent impact on the recipient environment. Adsorption of heavy metal ions in aqueous solutions has received increasing attention in recent years [9–11]. Low cost, regeneration of the adsorbent, high efficiency of heavy metal removal from diluted solutions, and the possibility of metal recovery are some of the major advantages of adsorption technique.

Mahakalkar et al. [12] studied the removal of iron from industrial and municipal waste water using non-activated carbon prepared from waste orange peel and obtained 51% removal, while activated carbon obtained from orange peel using HCl, HNO_3, and H_2SO_4 gave 91, 81, and 75% removal of iron, respectively. Iron removal efficiency of different samples of bamboo charcoals (i.e. *Bamboo balcooa*, *Bamboo mutans*, *Bamboo tulda* and *Bamboo padilla*) was inspected by Baruah et al. [13] and found the maximum removal of iron as 74.24, 59.46, 64.53, and 56.37%, respectively.

Removal of iron (III) from aqueous solution using polyacrylic acid hydrogel beads as adsorbent was carried out by Al-Abachi et al. [14]. They obtained maximum 59% removal in 24 h contact time at $400 \, mg \, dm^{-3}$ initial iron concentration.

In present work, we explore the novel sorbent nano-ZnO-loaded poly (acrylamide-co-itaconic acid) hydrogel (nano-ZnO-loaded PAI hydrogel), which has a high affinity for iron and fully exploit its ability in a wide range of metal concentrations. Nanoparticles of ZnO with high surface energy and surface area have strong adsorption capability. The removal efficiency was found to be more than 99%.

For the purpose of comparison of adsorption capacity of PAI hydrogel with and without nano-ZnO impregnation, the adsorption experiments were conducted. The PAI hydrogel loaded with nano-ZnO showed very high removal of iron (99%), whereas the adsorbent without nano-ZnO gave only 78.85% removal. Hence, impregnation of nano-ZnO particles improved the efficiency of the novel adsorbent in the removal of iron from aqueous solution. In the copolymer of acrylamide and itaconic acid, nano-ZnO particles were impregnated by in situ method because these nanoparticles have a tendency to aggregate, which reduces their high surface area to volume ratio and thus reduces the effectiveness of the nano-ZnO particles. Copolymer contains different functional groups which are involved in adsorption of iron and thus involve in removal of toxic iron from contaminated samples.

2. Experimental

2.1. Material

The monomers acrylamide and itaconic acid were purchased from Loba Chemi, Mumbai and Himedia, Mumbai, India, respectively. N,N´-methylene-bis-acrylamide (cross-linker) and potassium per sulfate (initiator) were purchased from Molychem, Mumbai, India. Triple distilled water was used throughout the experiments.

2.2. Synthesis of nano-ZnO-loaded PAI hydrogel

To a mixture of acrylamide and itaconic acid, the cross-linker (N,N´-methylene-bis-acrylamide) and initiator (potassium per sulfate) were added and heated at 70°C in an electric oven for 1 h. The copolymeric hydrogel so formed was washed with distilled water and cut into small uniform pieces. For in situ incorporation of nano zinc oxide particles within copolymeric matrix, these pieces were equilibrated in an aqueous

solution of zinc sulfate for 24 h. The Zn^{2+} loaded pieces of copolymer were then dipped in dilute NaOH solution and heated in an electric oven at 70°C for 4 h. The nano-ZnO-loaded copolymeric hydrogel was then washed thoroughly with distilled water, dried, and crushed into a fine powder.

2.3. Characterization of nano-ZnO-loaded PAI hydrogel

Nano-ZnO-loaded PAI hydrogel was characterized by TEM, SEM, Fourier transform infrared spectroscopy (FTIR), and AFM analysis.

2.3.1. TEM analysis

The average particle size, size distribution, and morphology of nano-ZnO particles were examined by TEM analysis (TECNAI—G20 TEM at a voltage of 200 kV). The solvent dispersion of the particles was drop—cast onto a carbon-coated copper grid and the grid was air dried at ambient conditions $(25 \pm 1°C)$ before loading into the microscope.

2.3.2. SEM analysis

To examine the morphological characteristics of nano-ZnO-loaded PAI hydrogel before and after iron adsorption, samples were viewed using a scanning electron microscope (SAIF, Punjab University, Chandigarh).

2.3.3. FTIR analysis

FTIR spectra of bare and iron loaded adsorbent were recorded using Varian Vertex FTIR Spectrometer. (UGC-DAE, Indore, India).

2.3.4. AFM analysis

The morphology and diameter of nano-ZnO particles were examined by contact mode AFM (NS-E, Digital Instrument Inc., USA) using silicon nitrate tip. The sample was prepared for AFM analysis by placing a few drops of the suspension of ZnO in distilled water on a cleaved mica sheet (UGC-DAE, Indore, India).

2.4. Preparation of stock solution

Stock solution of Fe(II) of 1,000 mg dm^{-3} was prepared by dissolving 0.179 g $(NH_4)_2Fe(SO_4)_2·6H_2O$ (AR) in 100 ml triple distilled water in 1% HNO_3 solution.

Suitable concentrations of Fe(II) for batch experiments were prepared by diluting the stock solution with triple distilled water.

2.5. Sampling

Sampling was performed as per the standard procedures and techniques to ensure representation of contaminated water samples and industrial effluent. Effluent sample was collected from drains coming out of the industrial site. In order to avoid the surface impurities, surface water samples were collected from about 40–50 cm below the surface. For sampling of contaminated water, polythene bottles were rinsed with 0.1 N HNO_3 and then washed twice with triple distilled water. In order to analyze the metal ions, samples were filtered and acidified with conc. HNO_3 to pH 2 and refrigerated at 4°C. For testing other parameters, virgin polythene cans were used for sample collection and analysis of samples was done within 48 h. Temperature, pH, and color of the samples were measured immediately after collection of samples at the sampling site by using thermometer, handy pH meter, and by visual observations, respectively.

2.6. Sample preparation

Digestion of contaminated water samples was carried out by standard APHA methods, which is necessary to destroy the organic contaminants, removal of ions that can interfere in analysis, because heavy metal ions have a tendency to form complexes with organic contaminants present in water samples. For digestion purpose, 50 ml of sample was heated with 10 ml conc. HNO_3 in fume cupboard. During heating, HNO_3 was added in small portions until the clear and light colored solution was obtained. The heating was continued till the volume was reduced to 10 ml, then allowed to cool, and volume was made to 50 ml with distilled water in standard flask and used for analysis.

2.7. Analytical technique

The concentration of iron was determined using Atomic Absorption Spectrometer (Varian AA-24-OFS model). Each experiment was carried out in triplicate under identical conditions to get the mean values.

2.8. Batch adsorption experiments

The adsorption experiments were carried out by batch method by varying contact time, pH, adsorbent

dose, adsorbate concentration, and temperature. For adsorption experiment, the nano-ZnO-loaded PAI hydrogel (0.1 g) and 20 ml iron solution of 10 mg dm^{-3} concentration at pH 4 and room temperature (25°C) was stirred for 50 min, which was found to be the sufficient time to attain equilibrium sorption. The amount of iron present in solution (before and after adsorption) was determined by Atomic absorption spectrometer.

The sorption degree (percentage removal) and sorption capacity of the sorbent were calculated by the following Eqs. (1) and (2), respectively:

$$\text{Sorption degree} = \frac{(C_0 - C_e)}{C_0} \times 100\% \qquad (1)$$

$$\text{Sorption capacity} = \frac{(C_0 - C_e) \cdot V}{m} \qquad (2)$$

where C_0 and C_e (mg dm^{-3}) are the initial and equilibrium concentrations of iron, respectively, V (L) is the volume of the iron solution subjected to sorption, and m (g) is the weight of sorbent.

2.9. Batch desorption experiments

For desorption, adsorbent loaded with iron was exposed to 20 ml of 0.1 M HNO$_3$ for a period of 24 h, centrifuged, and washed with triple distilled water. The adsorbent was then again exposed to HNO$_3$ to strip remaining iron and then reused.

2.10. Fixed-bed microcolumn adsorption experimental set up

Fixed-bed adsorption experiments were performed in a column made of polyethylene having an inner diameter of 0.5 cm and a height of 10 cm, at a constant temperature of 25°C. The column was packed with different bed heights of nano-ZnO-loaded PAI hydrogel on a glass-wool support. The experiments were performed at pH 4. The batch experimental results showed that the adsorption rate was high at pH 4. A known concentration of iron solution was allowed to pass through the bed at a constant flow rate (1 ml min^{-1}) in a downflow manner. For maintaining the constant flow rate of adsorbate solution the peristaltic pump was used. The iron solution was then collected at different time intervals, until the column reached exhaustion and the concentration of iron was determined by Atomic absorption spectrometer. The important design parameters such as column bed height, flow rate of metal solution into column, and

initial concentration of metal solution have been investigated.

2.11. Column desorption study

Column desorption study was carried out after the column adsorption studies were conducted, at 25 ± 0.2°C, using 0.1 M HNO$_3$ solution at flow rate of 1 ml min^{-1} and 2 cm bed depth to provide sufficient exchangeable H$^+$ ions for 330 min, and then washed with hot distilled water and could be reused for further adsorption experiment.

2.12. Adsorption kinetic studies

The kinetic investigations were carried out to measure the adsorption rate under various experimental conditions such as pH, temperature, and equilibrium time. For kinetic study, 0.1 g of adsorbent was shaken with 20 ml of iron solution of desired concentration and pH, using a temperature-controlled shaker on a constant agitation speed at different time intervals. The adsorbed amount of iron was calculated as adsorption equilibrium experiments.

3. Results and discussion

3.1. Characterization of nano-ZnO-loaded PAI hydrogel

The nano-ZnO-loaded PAI hydrogel was synthesized and characterized by the following instrumental methods.

3.1.1. TEM analysis

The shape, size, and morphology of nano-ZnO particles were determined through TEM imaging. The TEM images of nanoparticles show almost spherical zinc oxide particles with an average size of less than 20 nm, as shown in Fig. 1. Size of these nanoparticles lies within the range 10–20 nm. It should be noted, however, that the majority of the particles were scattered, a few of them showing aggregates indicate stabilization of the nanoparticles. The results represented by TEM images concluded that the particle size of individual nanoparticles seem to be 10–20 nm, whereas majority of nanoparticles exhibit smaller sizes, i.e. 11 and 14 nm.

3.1.2. SEM analysis

The SEM image of the sorbent surface is shown in Fig. 2 which clearly indicates the incorporation of ZnO-nano particles within copolymeric matrix. The
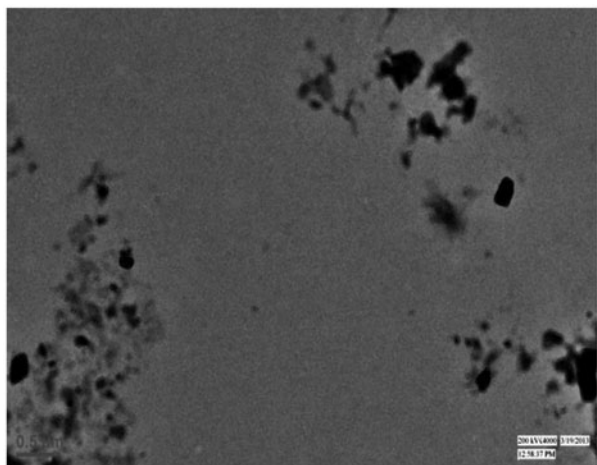
Fig. 1. Transmission electron micrograph of ZnO nanoparticles.

surface appears quit heterogeneous and uneven. The presence of large voids make the surface quit heterogeneous and porous, which justify significant adsorption capacity of sorbent.

3.1.3. FTIR analysis

FTIR of bare and iron adsorbed nano-ZnO-loaded PAI hydrogel are shown in Fig. 3(a) sample A and (b) sample B, respectively. The simultaneous presence of band in the regions 3,616–3,372 cm^{-1} is due to OH^- stretching of hydroxyl groups of carboxylic (–COOH) group. CH_2 (methylene group) stretching is obtained at 2,214.55 cm^{-1}. The FTIR analysis indicated the band due to acrylamide at 3,398 cm^{-1}, 1,659.18 cm^{-1}, 1,604 cm^{-1}, and 1,395.93 cm^{-1} attributed to N–H stretching, C=O stretching, N–H bending, and C–N stretching, respectively, which are the characteristics of the amide ($CONH_2$) group. Absorption peaks due

to itaconic acid were also observed at 1,725.86 cm^{-1} and 1,558.96 cm^{-1} for C=O and C–O stretching of the carboxylic (–COOH) group, respectively. The characteristic peak at 637.74 cm^{-1} relates to Zn–O group, which indicates the loading of nano-ZnO particles on PAI hydrogel because the surface of zinc oxide with negative charges has an affinity toward PAI hydrogel; the nano-ZnO particles could be loaded into protonated copolymer by the electrostatic interaction and chemical reaction through N,N´-methylene-bis-acrylamide cross-linking. In Fig. 3(b), a slight change in shape and intensity of absorbance (due to –$CONH_2$ and –COOH groups) has been noticed, which indicate that electron-rich nitrogen of amide group of acrylamide moiety and –COO^- group of itaconic acid moiety involve in removal of iron. Change in the peak position and intensity for Zn–O group stretching from 637.74 to 548.62 cm^{-1} indicate that iron coordinate with electron-rich oxygen of nano zinc oxide particles.

3.1.4. AFM analysis

The morphology of the nano-ZnO particles, using contact mode AFM, was found to be spherical having size distribution in two different diameter (height) ranges of 10–20 nm (mean height: 15 nm) and 50–120 nm (mean height: 60 and 90 nm) as shown in Fig. 4. However, some larger particle size in figure may be a result of agglomeration of smaller magnetite nanoparticles in order to reduce the inherent large surface energies for magnetite nanoparticles.

3.2. Adsorption isotherms

The adsorption isotherm indicates the distribution of adsorbed molecules between the liquid phase and solid phase when the adsorption process reaches an
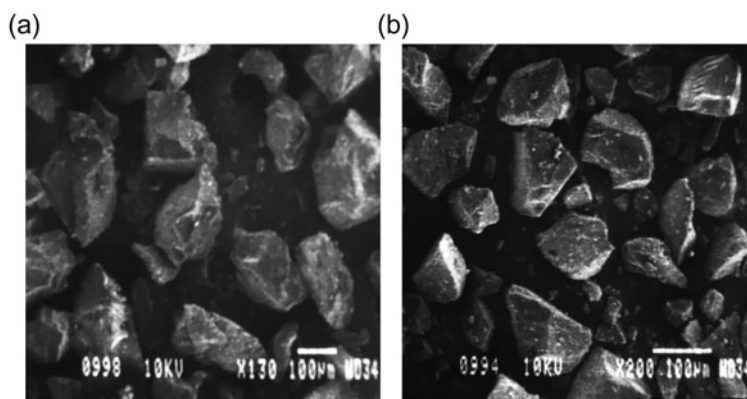

Fig. 2. SEM images of bare (a) ZnO nano particles loaded PAI hydrogel, (b) ZnO nanoparticles-loaded PAI hydrogel after iron adsorption.
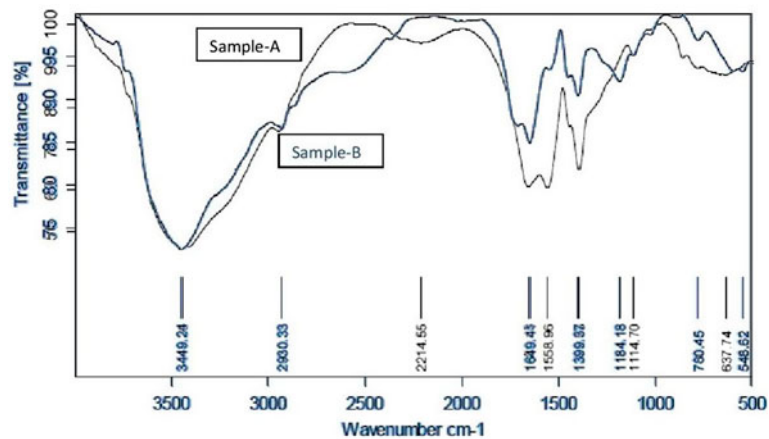
Fig. 3. FTIR pattern of (sample A) nano-ZnO-loaded PAI hydrogel before sorption of iron (sample B) nano-ZnO-loaded PAI hydrogel after sorption of iron.
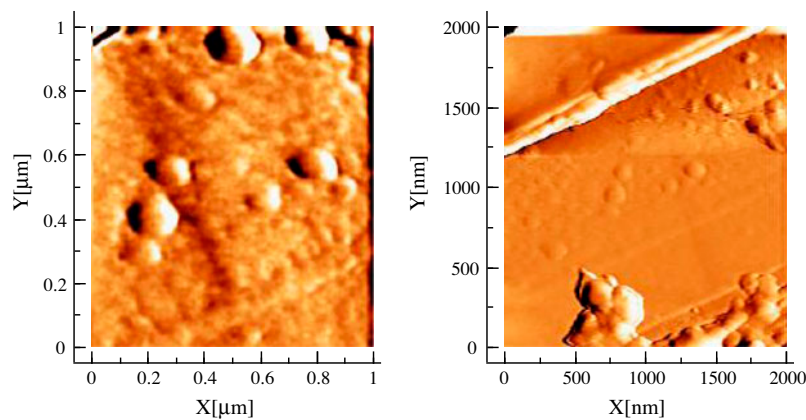

Fig. 4. AFM topographic images of ZnO nanoparticles on mica.

equilibrium state. The analysis of isotherm data by fitting them to different isotherm models is an important step in finding a suitable model that can be used for design purpose. The adsorption capacity of this system was investigated with the Freundlich and Langmuir adsorption isotherms.

3.2.1. Langmuir isotherm

The Langmuir sorption isotherm describes the surface as homogeneous, assuming that all the sorption sites have equal sorbate affinity and that adsorption at one site does not affect sorption at an adjacent site. The isotherm follows the typical Langmuir adsorption pattern as shown in Fig. 5. The linear form of the Langmuir isotherm may be represented as:
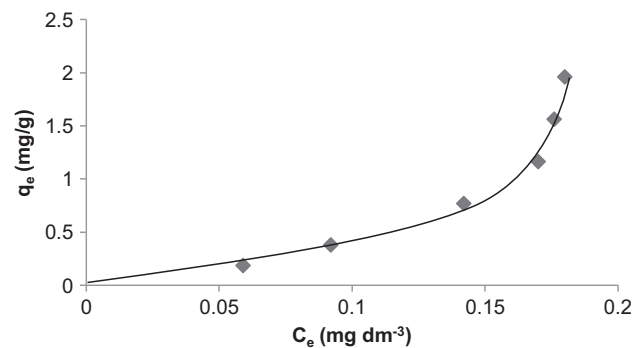

Fig. 5. Adsorption isotherm of nano-ZnO-loaded PAI hydrogel for iron.

Table 1
Constants of Langmuir, Freundlich, and Temkin isotherm models for iron

Langmuir constant			Freundlich constant			Temkin constant		
Q_o	b	R^2	K_f	n	R^2	a_s	b	R^2
−0.6234	−0.2506	0.979	0.0223	0.4417	0.976	3.7680	1.3410	0.791

$$\frac{C_e}{q_e} = b\frac{1}{Q_o} + \frac{C_e}{Q_o} \qquad (3)$$

where q_e is the amount of solute adsorbed per unit weight of adsorbent (mg/g), C_e is the equilibrium concentration of solute in the bulk solution (mg dm^{-3}), Q_o is the monolayer adsorption capacity (mg/g), and b is a constant related to free energy of adsorption. The values of Q_o and b can be calculated from the slope and intercept of the plot C_e/Q_e vs. C_e and shown in Table 1.

3.2.2. Freundlich isotherm

The Freundlich model is an empirical equation and can be applied for nonideal sorption on heterogeneous surfaces and multilayer sorption. The relation between the iron uptake capacity, q_e (mg/g) of adsorbent, and the residual iron concentration C_e (mg dm^{-3}) at equilibrium is given by the following equation:

$$\log q_e = \log K_f + \frac{1}{n}\log C_e \qquad (4)$$

where the intercept, $\log K_f$ is the measure of adsorbent capacity and the slope $1/n$ is the sorption intensity. The isotherm data fitted well in the Freundlich model ($R^2 = 0.976$). The values of constant K_f and n are given in Table 1. Since the value of n is less than 1, it indicates a favorable adsorption. The Freundlich isotherm is more widely used, but provides no information on the monolayer adsorption capacity, in contrast to the Langmuir model. The Freundlich isotherm is obeyed better than Langmuir isotherm, as is evident from the values of the adsorption capacities.

3.2.3. Temkin isotherm

The Temkin isotherm model is given by the following Equation:

$$X = a_s + b\ln C \qquad (5)$$

where C is the concentration of adsorbate in solution at equilibrium (mg dm^{-3}), X is the amount of metal adsorbed per unit weight of adsorbent (mg/g), a_s and b are the constants related to adsorption capacity and intensity of adsorption. The isotherm data fitted the Temkin equation poorly ($R^2 = 0.791$) than the Freundlich and Langmuir equations.

3.3. Adsorption kinetic modeling

The study of adsorption kinetics is important as it explains how fast the process occurs and also provides information on the factors affecting or controlling the adsorption rate. The progress of adsorption process was monitored at different time intervals (10–120 min), which clearly revealed that the adsorption of iron increased with increase in time and then leveled off after 50 min.

3.3.1. First-order reversible model

The sorption of iron from liquid to solid phase may be considered as a reversible reaction with an equilibrium state being established between the two phases. A simple first-order reaction model was, therefore, used to correlate the rates of reaction, which can be expressed by the following equation:

$$\ln[1 - U_{(t)}] = -k''t \qquad (6)$$

where k'' is the overall rate constant and calculated by following Equation:

$$k'' = k_1 + \left(1 + \frac{1}{K_c}\right) = k_1 + k_2 \qquad (7)$$

where k_1, k_2, and K_c are the forward, backward, and equilibrium rate constants, respectively, and can be obtained from the following Equation.

$$K_c = \frac{k_1}{k_2} = \frac{C_{Ae}}{C_e} \qquad (8)$$

Table 2
The first order reversible reaction rate constant for the removal of iron by nano-ZnO-loaded PAI hydrogel

Iron (mg dm^{-3})	Overall rate constant k'' = $k_1 + k_2$ (min^{-1})	Equilibrium constant K_c	Forward rate constant k_1 (min^{-1})	Backward rate constant k_2 (min^{-1})	Correlation coefficient R^2
10	0.023	135.99	0.0228	0.0002	0.989

$$U_{(t)} = \frac{X}{X_e} \tag{9}$$

where $U_{(t)}$ is called the fractional attainment of equilibrium. Therefore, a plot of ln $[1 - U_{(t)}]$ vs. time (min) will give a straight line. The overall rate constant k'' for a given concentration of iron was calculated by considering the slope of the straight line, and using Eqs. (7) and (8), the values of equilibrium constant K_c, forward, and backward rate constants k_1 and k_2 were calculated and are given in Table 2. From Table 2, it can be seen that the forward rate constant for the removal of iron is much higher than the backward rate constant, namely the desorption process. The uptake of iron by magnetic adsorbent was reversible and thus, has good potential for the removal/recovery of iron from aqueous solutions.

3.3.2. Second-order kinetics

The proposed second-order kinetic scheme is as follows:

Table 3
The second-order reaction rate constant for the removal of iron by nano-ZnO-loaded PAI hydrogel

Initial iron concentration (mg dm^{-3})	Second-order rate equation		Intraparticle rate constant k_p (mg^{-1} min$^{-1/2}$)
	k_2	R^2	
10	0.0246	0.987	0.006

$$\frac{1}{C} = k_2 \cdot \frac{t}{C_0} + \frac{1}{C_0} \tag{10}$$

where C and C_0 being the concentrations of metal ions in solution at any time t and zero time (i.e. initial concentration), respectively, and k_2 is the rate constant for adsorption. The value of k_2 is given in Table 3.

In order to examine the controlling mechanism of the adsorption processes, such as chemical reaction and mass transfer, the pseudo-first-order and pseudo-second-order equations were tested to model the kinetics of iron adsorption onto adsorbent.

3.3.3. Pseudo-first-order kinetics

Pseudo-first-order kinetic model was proposed by Lagergreen and the complete form of the model is

$$\log(q_e - q_t) = \log q_e - \frac{k_{ad}}{2.303} \cdot t \tag{11}$$

where q_t and q_e are the adsorption capacity (mg/g) at time t and at equilibrium, respectively, and k_{ad} is the pseudo-first-order rate constant of the adsorption. The rate constant k_{ad} and the correlation coefficient for iron adsorption at concentration 10 mg dm^{-3} were calculated from the linear plot of log $(q_e - q_t)$ vs. t, as listed in Table 4. The correlation coefficient for the pseudo-first-order kinetic model is low than that for pseudo-second order. Moreover, a large difference of equilibrium adsorption capacity (q_e) was found between the experimented and calculated result indicating a poor pseudo-first order fit to the experimental data.

Table 4
Comparison between the estimated adsorption rate constants, q_e and correlation coefficients associated with the pseudo-first-order and the pseudo-second-order rate equations

Initial iron concentration (mg dm^{-3})	Pseudo-first-order rate equation			Pseudo-second-order rate equation				
	k_{ad} (min^{-1})	q_e cal (mg/g)	R^2	k_2' (g mg^{-1} min^{-1})	q_e cal (mg/g)	R^2	h (mg g^{-1} min^{-1})	q_e exp (mg/g)
10	4.030	0.9772	0.992	1.848	1.988	0.999	7.303	1.985

3.3.4. Pseudo-second-order kinetics

The adsorption kinetics can also be characterized by a pseudo-second-order reaction. The linearized complete form of the model is given by

$$\frac{t}{q_t} = \frac{1}{k_2' q_t^2} + \frac{1}{q_e} t \tag{12}$$

where $k_2' q_t^2 = h$ (mg g^{-1} min^{-1}) can be considered as the initial adsorption rate when $t \rightarrow 0$ and k_2' (g/mg min) is the pseudo-second-order rate constant. The plot of t/q_t vs. t should give a straight line; if pseudo-second-order kinetics is applicable, then q_e, k_2', and h can be resolved from the slope and intercept of plot, respectively. At initial iron concentration (10 mg dm^{-3}), a straight line with extremely high correlation coefficient ($R^2 = 0.999$) was obtained. In addition, the calculated q_e value also consents with the experimental data in the case of pseudo-second-order kinetics, as shown in Table 4. This suggests that the adsorption data are well defined by pseudo-second-order kinetics and approved the hypothesis that rate-limiting step of iron adsorption on nano-ZnO-loaded PAI hydrogel may be a chemical sorption. In chemisorption, the metal ions adhere to the adsorbent surface by producing a chemical (usually covalent) bond and tend to find sites that increase their coordination number with the surface [15].

3.3.5. Intra particle diffusion

Besides adsorption at the outer surface, there is also a possibility of intraparticle diffusion from the outer surface into the pores of adsorbent material. The mechanism of adsorption of sorbate onto the adsorbent follows three steps viz. film diffusion, pore diffusion, and intraparticle transport [16]. Though there is a high possibility of pore diffusion to be the rate-limiting step in a batch process, the adsorption rate parameter which governs the batch method for most of the contact time, is the intra particle diffusion. Thus, in order to evaluate the rate-controlling step a plot was drawn between the amounts of iron adsorbed on magnetic adsorbent (a) vs. $t^{1/2}$. The rate constant for intraparticle diffusion is attained using the following equation:

$$q_t = k_p t^{1/2} \tag{13}$$

where k_p is the intraparticle diffusion rate constant (mg^{-1} min$^{-1/2}$). The value of k_p was determined from the slope of linear portion of curve which is given in Table 3.

3.4. Thermodynamic study

Thermodynamic parameters such as free energy ($\Delta G°$), enthalpy ($\Delta H°$), and entropy ($\Delta S°$) change of adsorption can be evaluated from the below equation:

$$K_c = \frac{C_{Ae}}{C_e} \tag{14}$$

where K_c is the equilibrium constant, C_e is the equilibrium concentration of solution (mg dm^{-3}), and C_{Ae} is the solid-phase concentration at equilibrium (mg dm^{-3}). The K_c values are used to determine $\Delta G°$, $\Delta H°$, and $\Delta S°$.

$$\Delta G° = -RT\,2.303 \log K_c \tag{15}$$

where $\Delta G°$ is the free energy of adsorption (kJ/mol), T is absolute temperature (Kelvin), and R is the universal gas constant (8.314 J/mol/K).

The K_c may be expressed in terms of the $\Delta H°$ (kJ/mol) and $\Delta S°$ (J/mol/K) as a function of temperature.

$$\log K_c = \frac{\Delta S°}{2.303\,R} - \frac{\Delta H°}{2.303\,RT} \tag{16}$$

According to Eq. (16), the values of $\Delta H°$ and $\Delta S°$ were determined from the slope and the intercept of the plot of $\log K_c$ vs. $1/T$. The $\Delta G°$ values were calculated by Eq. (15). Adsorption of iron on nano-ZnO-loaded PAI hydrogel decreased with the increase in temperature from 298 to 328 K as shown in Fig. 9. The process was thus observed to be exothermic in nature. The plot was used to compute the values of the thermodynamic parameters, as shown in Table 5. The values of the enthalpy change ($\Delta H°$) and the entropy change ($\Delta S°$) were found to be −38.33 kJ/mol and −0.090 J/mol/K, respectively, for 10 mg dm^{-3} iron concentration. The negative $\Delta G°$ value indicates that the process is feasible and the adsorption is spontaneous in nature. The negative $\Delta H°$ value indicates the exothermic nature of adsorption, and the negative value of $\Delta S°$ suggests a decrease in the randomness at the solid/solution interface during the adsorption of iron onto adsorbent.

It has been reported that $\Delta G°$ values up to −20 kJ/mol are consistent with electrostatic interaction between sorption sites and the metal ions (physical adsorption), while $\Delta G°$ values more negative than −40 kJ/mol involve charge sharing or transfer from the adsorbent surface to the metal ion to form a coordinate bond (chemical adsorption) [17]. The $\Delta G°$ values obtained in this study

Table 5
Thermodynamic parameters for the adsorption of iron onto nano-ZnO-loaded PAI hydrogel

Initial iron concentration (mg dm^{-3})	$\Delta H\degree$ (kJ/mol)	$\Delta S\degree$ (J/mol/K)	$\Delta G\degree$ (kJ/mol)			
			25℃	35℃	45℃	55℃
10	−38.33	−0.090	−11.880	−10.256	−9.417	−9.160

for iron adsorption are < −11.880 kJ/mol, which indicates that physical adsorption is the predominant mechanism in the sorption process [18].

3.5. Factors affecting adsorption

3.5.1. Effect of contact time

The adsorption of iron increased with increasing contact time and become almost constant after 50 min. From Fig. 6, the plot reveals that the percent iron removal is higher at the beginning; this is probably due to a larger surface area of the adsorbent being available at the beginning for the adsorption of iron. As the surface adsorption sites become exhausted, the uptake rate is controlled by the rate at which the adsorbate is transported from the exterior to the interior sites of the adsorbent particles. Further increase in contact time did not increase the uptake due to deposition of metal ions on the available adsorption sites on the adsorbent material. Thus, 50 min has been observed to be optimum contact time for the maximum removal of iron using nano-ZnO-loaded PAI hydrogel.

3.5.2. Effect of pH

The pH of the aqueous solution is an important controlling parameter in the adsorption process and influence the removal efficiency of the mercury. In order to study the effect of hydrogen ion concentration on the removal of iron, the adsorption experiments were performed at different pH levels ranging from 2 to 8, using 0.1 M HNO$_3$ and 0.1 M NaOH for adjusting the solution pH. It was observed that with the increase in pH (from 2 to 4) the percentage removal of iron increased and decreased after pH 4 (shown in Fig. 7). The observed increase may be due to the decrease in competition between proton and metal cations for same functional groups and decrease in positive surface charges, which results in a lower electrostatic repulsion between surface and metal ions.
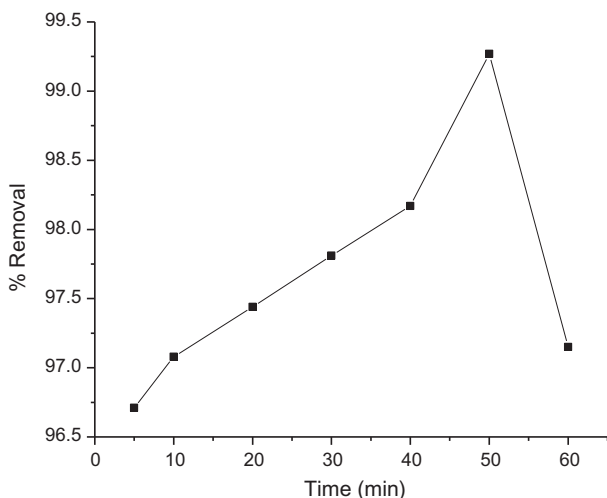

Fig. 6. Effect of time variation on iron removal through nano-ZnO-loaded PAI hydrogel = 0.1 g, pH 4, temp. = 25 ± 0.2℃.
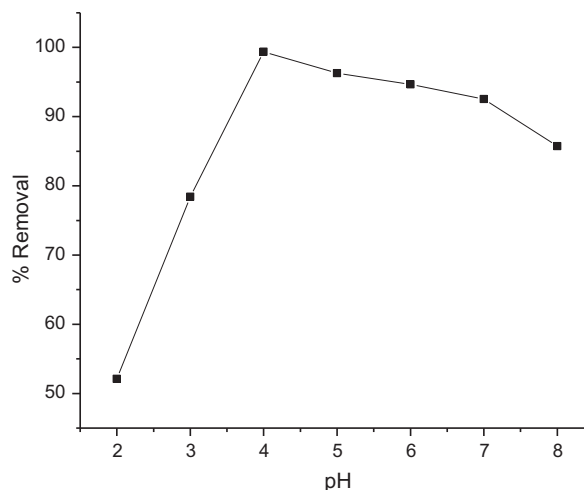

Fig. 7. Effect of pH variation on iron removal through nano-ZnO-loaded PAI hydrogel = 0.1 g, time = 50 min, temp. = 25 ± 0.2℃.

The highest uptake of iron was obtained at pH 4 and at pH values higher than 8, metal precipitation occurred and adsorption capacity was decreased with accumulation of metal ions. Therefore, an optimum pH 4 was selected for adsorption experiments.

3.5.3. Effect of adsorbent dosage

The dependence of iron sorption on adsorbent dose was studied by varying the amount of nano-ZnO-loaded PAI hydrogel from 0.04 to 0.1 g with fixed volume of adsorbate (20 ml) keeping other parameters like pH, contact time, and temperature constant. It was noticed that maximum removal of iron was obtained with 0.1 g adsorbent and any further addition of the adsorbent did not cause any significant change in the removal of iron, as shown in Fig. 8. The observed increase in uptake (0.04–0.1 g adsorbent dose) may be due to the availability of more binding sites on adsorbent and decreases after the saturation, hence the amount of ions bound to the adsorbent, and amount of free ions remain constant; even with further addition of dose of adsorbent.

3.5.4. Effect of temperature

The temperature plays an important role on retention of metal ions by adsorbent. Effect of temperature on removal of iron was studied by conducting adsorption experiments at different temperatures ranging from 25 to 55℃ and the maximum uptake of iron was obtained at 25℃, which then decreases with the
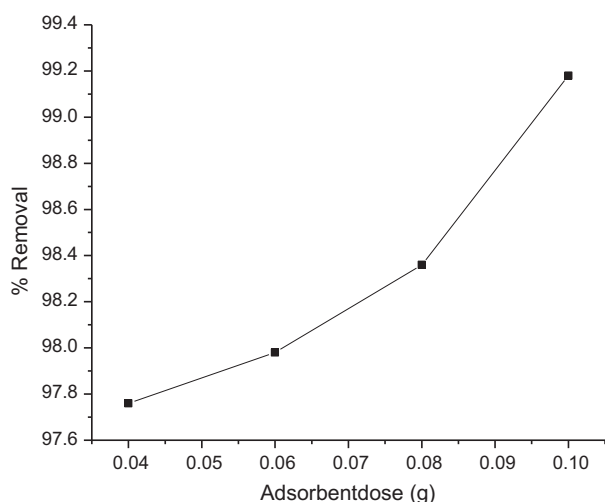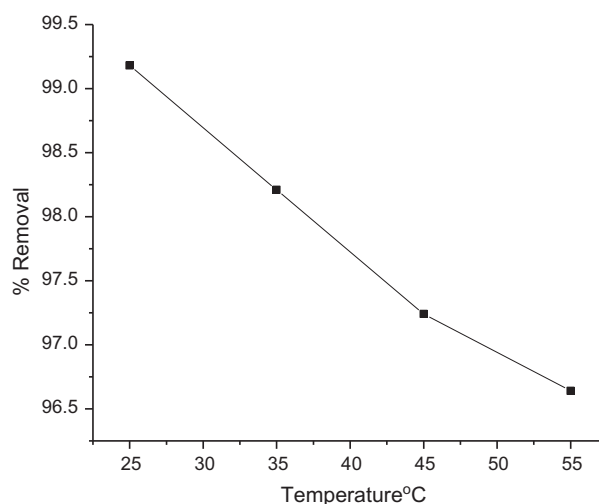

Fig. 9. Effect of temperature variation on iron removal through nano-ZnO-loaded PAI hydrogel = 0.1 g, pH 4, and time = 50 min.

increase in temperature as shown in Fig. 9. The decrease in iron removal may be due to the weakening of binding forces between iron and active sites on the copolymer. This is mainly due to the decreased surface activity, suggesting that the process of adsorption between iron and adsorbent is an exothermic process.

3.5.5. Effect of initial concentration of iron

The effect of initial concentration on removal of iron by nano-ZnO-loaded PAI hydrogel was studied by performing the adsorption experiments with different iron concentrations ranging from 1 to 10 mg dm^{-3} and it was observed that with the increase in adsorbate concentration, the percentage removal of iron increase, as shown in Fig. 10. The observed increase is quite obvious, as on increasing the concentration of solute, greater numbers of metal ions arrive at the interface and thus, get adsorbed.

3.6. Fixed-bed microcolumn adsorption experiments

The maximum percentage removal of iron using fixed-bed microcolumn of nano-ZnO-loaded PAI hydrogel was found to be increased with the increase in bed depth, and initial metal ion concentration and decreased with the increase in feed flow rate. The highest percentage removal was obtained at 1 ml min^{-1} flow rate, 2 cm bed depth and 10 mg dm^{-3} inlet iron concentration at pH 4 and 25℃ temperature. It was observed that equilibrium metal uptake (q_0)

Fig. 8. Effect of adsorbent dose variation on iron removal through nano-ZnO-loaded PAI hydrogel pH 4, time = 50 min, temp. = 25 ± 0.2℃.

increased with increase in flow rate and inlet iron concentration and decreased with increase in bed depth. Both breakthrough point and exhaustion time increased with increase in bed depth and inlet iron concentration and decreased with increase in flow rate.
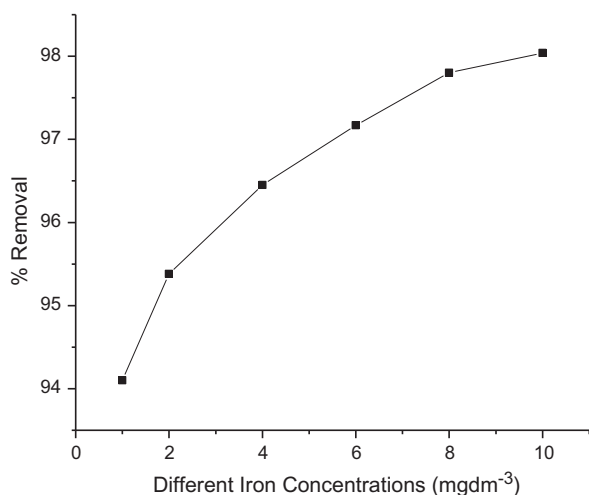

Fig. 10. Effect of different concentration on iron removal through nano-ZnO-loaded PAI hydrogel = 0.1 g, pH 4, time = 50 min, and temp. = 25 ± 0.2 °C.

3.7. Column desorption study

Desorption results indicated 99.50% recovery of iron from the surface of the sorbent using 0.1 M HNO_3 in 330 min at 25 °C temperature. The nano-ZnO-loaded PAI hydrogel showed almost the same metal ion adsorption capacity after the repeated regeneration. It may be stated that, in acidic medium, protons compete with iron and displace the maximum amount of adsorbed iron. Hence, ion-exchange mechanism is important in connection with adsorption–desorption process for adsorbent.

3.8. Mechanism of uptake

The nano-ZnO-loaded PAI hydrogel contains carboxyl and amide groups as confirmed by FTIR analysis are responsible for binding the toxic iron on the surface. The proposed mechanism of binding the iron on various sites available at adsorbent surface (Fig. 11) may be explained as follows.

(a) Carboxylate groups ($–COO^-$) of itaconic acid moiety of copolymer interact with iron.
(b) Iron coordinate with the electron-rich nitrogen of amide group of acrylamide moiety of copolymer.
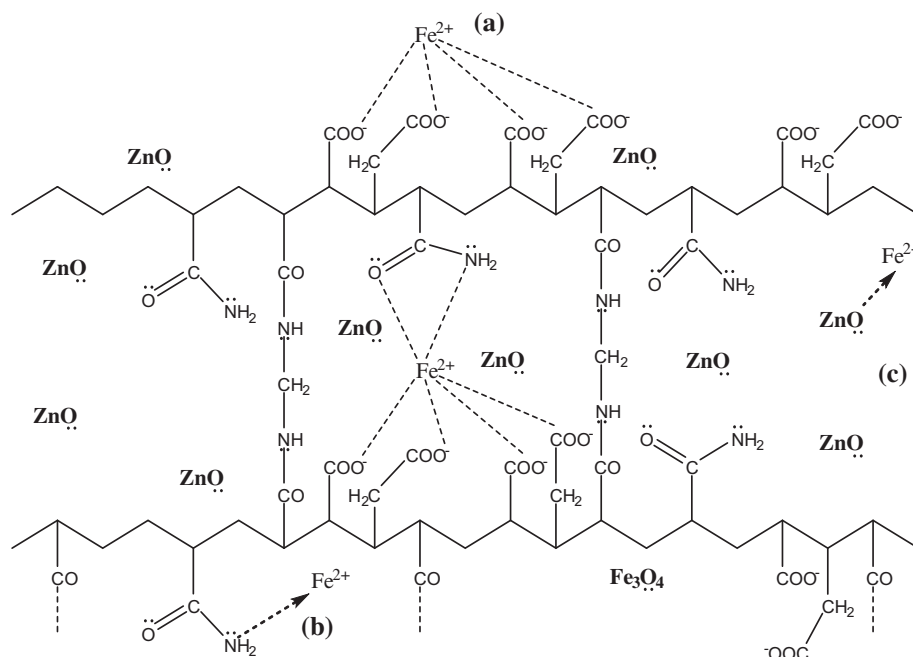

Fig. 11. Scheme of mechanism of iron uptake by nano-ZnO-loaded PAI hydrogel through co-ordination with (a) carboxylate groups of itaconic acid moiety, (b) electron-rich amide group of acrylamide moiety, and (c) electron-rich oxygen of nano-ZnO particles.

Table 6
Application of nano-ZnO-loaded PAI hydrogel in the removal of iron from Shankhini River (Dantewada, Chhattisgarh, India) using nano-ZnO-loaded PAI hydrogel = 0.1 g, pH = 4 time = 50 min, temperature = 25 ± 0.2°C in batch system and 2 cm bed depth, 1 ml min-1 feed flow rate in column system

Name of adsorbents	Name of metal ions	Concentration of iron in Shankhini River water (mg dm^{-3})	% Removal in batch adsorption system	% Removal in column adsorption system
Nano-ZnO-loaded poly (acrylamide-co-itaconic acid) hydrogel	Iron	1.8000	99.50	99.86

Table 7
Application of nano-ZnO-loaded PAI hydrogel in the removal of iron from metal polishing industrial effluent

Name of adsorbents	Name of metal ions	Concentration of iron in contaminated water (mg dm^{-3})	% Removal in batch adsorption system	% Removal in column adsorption system
Nano-ZnO-loaded poly (acrylamide-co-itaconic acid) hydrogel	Iron	8.0236	98.34	98.58

(c) In addition within the copolymer matrix, these irons may also coordinate with the electron-rich oxygen of nano-ZnO particles.

3.9. Application part

The metal polishing industrial wastewater and contaminated surface and ground water samples were collected, and the optimized conditions as set in batch as well as column techniques for maximum removal of toxic metal ions were applied, to get the pure water for drinking and other purposes.

3.9.1. Removal process

(a) For batch adsorption study 20 ml sample water was shaken with 0.1 g of nano-ZnO-loaded PAI hydrogel for 50 min at 4 pH and room temperature (25°C). The amount of iron present in sample (before and after adsorption) was determined by Atomic absorption spectrometer.
(b) For column adsorption study contaminated water was allowed to pass through 2 cm column filled with nano-ZnO-loaded PAI hydrogel at 1 ml min^{-1} feed flow rate. The iron solution was then collected at different time intervals till the exhaustion of column and the concentration of iron was determined by Atomic absorption spectrometer.

Tables 6 and 7 show the results of iron removal from Shankhini River (Dantewada, Chhattisgarh, India) and metal polishing industrial wastewater, respectively.

4. Conclusion

The nano zinc oxide loaded PAI hydrogel has been found to be an effective, efficient, and a cheap adsorbent for high removal of iron from aqueous solution as well as contaminated water by batch and column methods. The maximum percentage removal (<99%) was obtained at 4 pH and 25°C temperature in 50 min. The equilibrium sorption data fitted the Freundlich model better than Langmuir and Temkin isotherm models. Thermodynamic parameters depicted the exothermic nature of adsorption and a favorable process for iron removal. The pseudo-second-order reaction rate model described the kinetic data best for iron adsorption. The nano-ZnO-loaded PAI hydrogel could be repeatedly used in the adsorption studies by adsorption–desorption cycle without detectable losses in their initial adsorption capacities. Since this method involves less capital cost and is highly efficient, it is practically feasible for the removal of poisonous metal ions from industrial effluents as well as contaminated ground/surface water to make the water safe for drinking and other purposes. The calculated column parameters could be scaled up for the design of fixed-bed columns for effective and efficient removal of toxic metal ions from water.

References

[1] J. Kyziol-Komosinska, F. Barba, P. Callejas, C. Rosik-Dulewska, Beidellite and other natural low-cost sorbents to remove chromium and cadmium from water and wastewater, Bol. Soc. Esp. Ceram. 49 (2010) 121–128.

[2] S.K. Papageorgiou, F.K. Katsaros, E.P. Kouvelos, N.K. Kanellopoulos, Prediction of binary adsorption isotherms of Cu^{2+}, Cd^{2+} and Pb^{2+} on calcium alginate beads from single adsorption data, J. Hazard. Mater. 162 (2009) 1347–1354.

[3] H.V. Jadhav, Element of Environmental Chemistry, Himalaya Publishing Home, Mumbai, 1992.

[4] Y.L. Lai, M. Thirumavalavan, J.F. Lee, Effective adsorption of heavy metal ions (Cu^{2+}, Pb^{2+}, Zn^{2+}) from aqueous solution by immobilization of adsorbents on Ca-alginate beads, Toxicol. Environ. Chem. 92 (2010) 697–705.

[5] R.M.P. Silva, J.P.H. Manso, J.R.C. Rodrigues, R.J.J. Lagoa, A comparative study of alginate beads and an ion-exchange resin for the removal of heavy metals from a metal plating effluent, J. Environ. Sci. Health, Part A 43 (2008) 1311–1317.

[6] P.D. Nemade, A.M. Kadam, H.S. Shankar, Removal of iron, arsenic and coliform bacteria from water by novel constructed soil filter system, Ecol. Eng. 35 (2009) 1152–1157.

[7] G. Anusha, Removal of iron from wastewater using bael fruit shell as adsorbent, 2nd International Conference on Environmental Science and Technology, IPCBEE 6, IACSIT Press, Singapore, 2011, pp. 258–260.

[8] S. Borhade, Synthesis, characterization and spectrophotometric determination of Fe(II) complex of 2,4-dihydroxybenzaldehyde isonicotinoyl hydrazone {(E)-N´-(2,4-dihydroxybenzylidene) isonicotinohydrazide, it's application & biological activity, Der. Chemica. Sin. 2 (2011) 64–71.

[9] Y. Kaçar, Ç. Arpa, S. Tan, A. Denizli, Ö. Genç, M.Y. Arıca, Biosorption of Hg(II) and Cd(II) from aqueous solutions: comparison of biosorptive capacity of alginate and immobilized live and heat inactivated *Phanerochaete chrysosporium*, Process Biochem. 37 (2002) 601–610.

[10] R.S. Bai, T.E. Abraham, Studies on chromium (VI) adsorption–desorption using immobilized fungal biomass, Bioresour. Technol. 87 (2003) 17–26.

[11] F.A. Al-Rub, M.H. El-Naas, F. Benyahia, I. Ashour, Biosorption of nickel on blank alginate beads, free and immobilized algal cells, Process Biochem. 39 (2004) 1767–1773.

[12] A.S. Mahakalkar, S.N. Nandeshwar, R.R. Gupta, Removal of iron from industrial and municipal waste water using low cost adsorbent prepared from waste orange peel, Arch. Appl. Sci. Res. 6 (2014) 26–35.

[13] B.K. Baruah, B. Das, A. Haque, K. Misra, A.K. Misra, Iron removal efficiency of different bamboo charcoals: A study on modified indigenous water filtration technique in rural areas of Assam, J. Chem. Pharm. Res. 3 (2011) 454–459.

[14] M.Q. Al-Abachi, N.S. Al-Awady, A.M. Al-Anbakey, Removal of iron (III) ion from aqueous solution using polyacrylic acid hydrogel beads as adsorbent, Iraqi J. Sci. 54 (2013) 775–781.

[15] P.W. Atkins, Physical Chemistry, Oxford University Press, Oxford, 1995.

[16] K.K. Pant, T.S. Singh, Equilibrium kinetics and thermodynamic studies for adsorption of As (III) on activated alumina, Sep. Purif. Technol. 36 (2004) 139–147.

[17] M. Horsfall, A.I. Spiff, A.A. Abia, Studies on the influence of mercaptoacetic acid (MAA) modification of cassava (manihot sculenta cranz) waste biomass on the adsorption of Cu^{2+} and Cd^{2+} from aqueous solution, Bull. Korean Chem. Soc. 25 (2004) 969–976.

[18] N.T. Abdel Ghani, G.A. Elchaghaby, Influence of Cu, Zn, Cd and Pb ion from wastewater by adsorption, Int. J. Environ. Sci. Technol. 4 (2007) 451–456.